Journal of Thermal Science Vol.22, No.6 (2013) 539–546

DOI: 10.1007/s11630-013-0660-8 **Article ID: 1003-2169(2013)06-0539-08**

Performance Improvements of a Subsonic Axial-Flow Compressor by Means of a Non-Axisymmetric Stator Hub End-Wall

ZHANG Xuefeng [1, 2], LU Xingen [1], ZHU Junqiang [1]

1. Key Laboratory of Light-duty Gas-turbine, IET, CAS, Beijing 100190, China
2. Graduate School of Chinese Academy of Sciences, Beijing, 100190, China

This paper deals with the application of a non-axisymmetric hub end-wall on the stator of a single stage high subsonic axial-flow compressor. In order to obtain a state-of-the-art stator non-axisymmetric hub end-wall configuration fulfilling the requirements for higher efficiency and total pressure ratio, an automated multi-objective optimizer was used, in conjunction with 3D-RANS-flow simulations. For the purpose of quantifying the effect of the optimal stator non axis-symmetric hub contouring on the compressor performance and its effects on the subsonic axial-flow compressor stator end-wall flow field structure, the coupled flow of the compressor stage with the baseline, axisymmetric and the non-axisymmetric stator hub end-wall was simulated with a state-of-the-art multi-block flow 3D CFD solver. Based on the CFD simulations, the optimal compressor hub end-wall configuration is expected to increase the peak efficiency by approximately 2.04 points and a slight increase of the total pressure ratio. Detailed analyses of the numerical flow visualization at the hub have uncovered the different hub flow topologies between the cases with axisymmetric and non-axisymmetric hub end-walls. It was found that that the primary performance enhancement afforded by the non-axisymmetric hub end-wall is a result of the end-wall flow structure modification. Compared to the smooth wall case, the non-axisymmetric hub end-wall can reduce the formation and development of in-passage secondary flow by aerodynamic loading redistribution.

Keywords: Axial-flow compressor; Non-axisymmetric end-wall; Numerical simulation

Introduction

Secondary flows involving cross flow and three-dimensional separation phenomena contribute greatly to passage blockage, which effectively places a limit on the loading and static pressure rise achievable by the compressor. In addition, the subsequent mixing of the flow in the separated region with the main passage flow may lead to a considerable total pressure loss and a consequent reduction in compressor efficiency. If these secondary flows can be decreased in size and strength, then their associated losses will also decrease. So, specific strategies for reducing or eliminating the passage secondary flows such as leading edge fillet, end-wall contouring and 3D-blading (altering rotor and stator blade shapes) have been explored [1-5]. Recent investigations [6-7] have shown that relatively local geometric design modification at the hub or tip end-walls yield a significant reduction of secondary flow loss. So far, more and more attention is focused on loss reduction and performance improvement through optimization of end-wall. For example, various types of casing treatment means such as slots or grooves cut into the compressor casing above the rotor end-wall have been used to control the end-wall flow and alleviate

Received: May 2013 Xingen Lu: Associate Professor
Financial support for the work presented is provided by National Natural Science Foundation of China (Project No: 51176187)

the stall phenomena, therefore improve the compressor's stall margin [8-10].

Another interesting approach to control end-wall secondary flow is the use of non-axisymmetric end-wall, here the end-wall no longer remains axisymmetric but has a changing profile in the blade-to-blade direction, which provides additional degrees of freedom for compressor geometric set-ups. To date, the non-axisymmetric end-wall has been shown to be a powerful method to improve the aerodynamic efficiency of axial turbines [11-13]. However, concerning axial compressors, this approach is still a field of research and only a few attempts have been made till now [14-16]. Although many research projects have been carried out with the goal to understand the specific impact on the compressor flow, many basic questions are still unsolved. So far, there are no design guidelines which allow to design and to adapt a specific non-axisymmetric end-wall to the individual aerodynamic requirements of a compressor stage. Researchers have explored several different contouring methods but much work remains before the concept is perfected.

This paper deals with the application of a non-axisymmetric hub end-wall to a high subsonic axial-flow compressor stator. An automated multi-objective optimizer in conjunction with 3D RANS flow solver was used to find the optimal hub end-wall geometries concerning the performance of compressor. Hereafter, the effect of non-axisymmetric hub contouring on the compressor performance was quantified and the resulting flow phenomena and physics due to the modified end-wall surface were analyzed in detail. The goal of this paper is to explore strategies for reducing secondary flows in blade passages through the use of asymmetric end-wall contouring which would provide additional degrees of freedom for compressor geometric set-ups.

Investigated Compressor and Description of the Numerical Model

A single stage high subsonic axial-flow compressor at the Northwestern Poly-technical University (NWPU), which is conceived as a fundamental research stage, has been selected as the test bed for the non-axisymmetric profiled end-walls investigation and optimization based on numerical results. The detailed aerodynamic design parameters of the compressor stage are presented in Table 1. Further detailed information of this compressor can be found in References 17 through 19.

Computation was done for three-dimensional flow using the Navier-Stokes solver EURANUS [20]. The Favre-Reynolds averaged Navier-Stokes equations were discretized using a cell-centered explicit finite volume scheme according to Jameson in a relative coordinate system rotating with the reference frame. The steady-state flow solution was achieved at the convergence of a four-stage explicit Runge-Kutta integration scheme. The time marching algorithm was stabilized using scalar eigenvalue-based second- and fourth-order difference smoothing operators. In order to speed up convergence to steady state, local time stepping, residual smoothing, and multi-grid techniques were applied. The one-equation Spalart-Allmaras turbulence model was applied for turbulence closure.

Table 1 Design Specifications of a Compressor Stage

Quantity	Value
Corrected mass flow (kg/s)	5.6
Total-to-total pressure ratio	1.249
Inlet relative Mach number at tip	0.78
Shaft speed (r/min)	15200
Corrected tip speed (m/s)	237
Number of rotor blades	30
Number of stator blades	44
Rotor tip diameter (mm)	298
Rotor hub-tip ratio	0.61
Nominal tip clearance (mm)	0.3
Rotor mean aspect ratio	0.94
Rotor solidity (tip)	0.96
Stator mean aspect ratio	1.86
Stator solidity (tip)	1.4

To evaluate properly the viscous fluxes at the walls using the chosen boundary conditions (no-slip, adiabatic wall condition without a wall function method), the distance away from the wall of the first node had to be judiciously determined. This became an important grid parameter. In this work, the grids were meshed ensuring y+ of the first layer node was equal to or smaller than 2 by setting the maximum distance between the wall and first node.

No-slip and no-heat transfer conditions were imposed at solid boundaries. At the inflow boundary of the rotor, flow angle, total pressure and total temperature were prescribed according to the experimental data. At the subsonic outlet, static pressure was prescribed at the hub and its radial variation calculated based on the radial equilibrium equation.

Design of Non-Axisymmetric Hub End-wall via Optimization

The objective for the asymmetrically contoured end-wall was to reduce the cross passage pressure gradient, creating weaker cross flows and secondary flows. The basic idea for doing this is to raise the end-wall near

the pressure side of the blade with convex curvature and lower the end-wall near the suction side with concave curvature.

In the present work, CFD-based non-axisymmetric end-wall shape optimization has been used to obtain a state-of-the-art geometry of the stator's hub surface concerning the rise in efficiency and pressure ratio. For this purpose the flow solver Fine/Turbo by NUMECA was used. This optimization strategy was based on a multi-objective evolutionary algorithm which uses self-learning neural networks being fed by a previously generated database of arbitrary geometries each with the corresponding own performance. Detailed descriptions of the multi-objective optimization tools used can be found in Reference 20.

Non-axisymmetric hub end-wall design requires a novel surface design algorithm. It uses B-Spline curves and tensor product surfaces in order to meet parameterization standards inside the process-chain. Fig.1 visualizes this described parameterization area within the row and a certain variety of symbols for specific control points. To parameterize the end wall perturbation area, cuts were built along a virtual stream-line which is aligned with the blade camber curve as shown in Fig. 1(a). The blade channel was divided into 5 cuts, each with a distance of 25% of the blade channel width. A uniform distribution of 4 parameters was selected along the cuts. In the circumferential direction, the perturbation law is defined by Bezier curves controlled by height parameters as shown in Fig. 1(b). To ensure slope continuity, the additional values h1 and h5 in Fig.1 were automatically managed by the algorithm and could not be accessed by the user. Furthermore, an axis-asymmetric end-wall modification for a single blade row at end-wall should be possible without altering the entire compressor end-walls. Therefore, the 3D design space was limited to the flow channel of a blade row which is created by the blade surfaces and surfaces of the gas path annulus. At the inlet and outlet interfaces of a blade row, the modified end-wall has to be geometrically continuous with the symmetric end-wall in order to fit to the existing compressor. Additionally, start and end cuts must be identical to ensure geometric continuity. The final parameterized patch was a loft surface passing through the perturbed cuts. For the optimization, all parameters were varied between –2.5 mm to 2.5 mm in the radial direction. This corresponded to 5% of the stator channel height. This finally led to 16 free parameters for the optimization, which requires approximately 35–45 samples in the initial database. The objectives of optimization were improving design efficiency while maintaining or improving design point pressure ratio.

The convergence history of the optimization procedure is shown in Fig.2, one can observe that the error between the neural network predictions and the CFD results decrease, both curves finally converging after some 20 iterations.

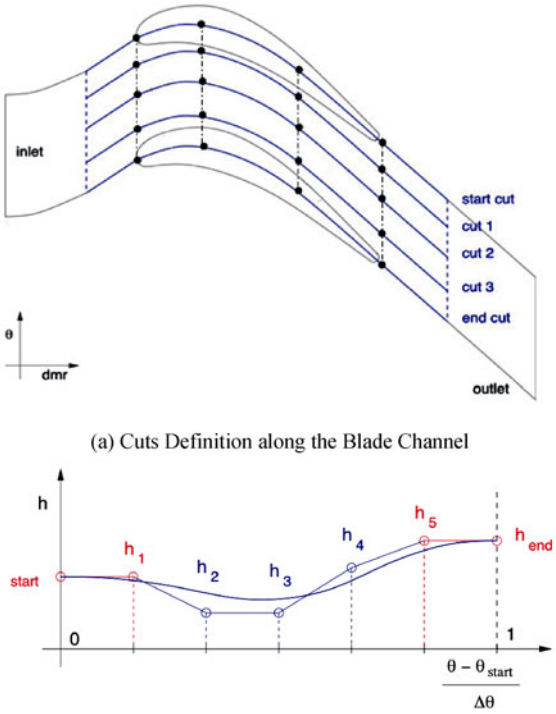

(a) Cuts Definition along the Blade Channel

(b) Circumferential Pertur bation Law for the Blade Channel

Fig.1 Distribution of Non-Axisymmetric Hub End-Wall Control Points

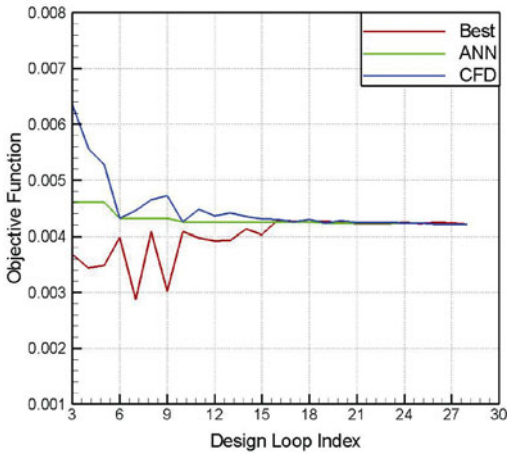

Fig.2 Evolution of Objective Function during Optimization

The final profiled end-wall chosen for the detailed numerical study was based on an optimized non-axisymmetric hub end-wall configuration after 25 optimization cycles that provide the best compressor performance. An isometric view of the non-axisymmetric contoured end-wall profile and non-axisymmetric profile height contours employed at the bottom end-wall for the present computations in the blade passage is shown in Fig.3,

where height = 0.0 mm refers to the location of the baseline, axisymmetric end-wall. The shroud end-wall remains always axisymmetric without any contouring as mentioned earlier. The maximum height of the complete profile is located slightly upstream of the trailing edge. The lowest trough in the profile is located mid pitch near the blade trailing.

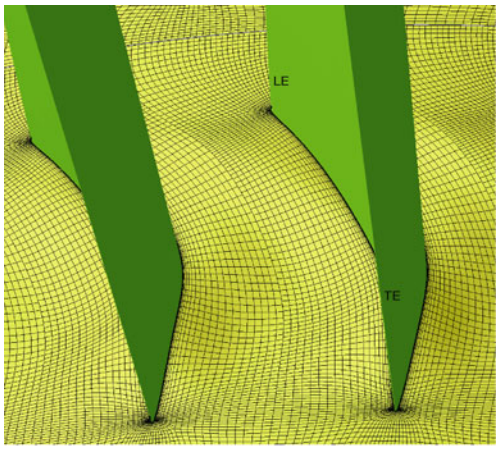

(a) Isometric View of Stator Hub End-Wall

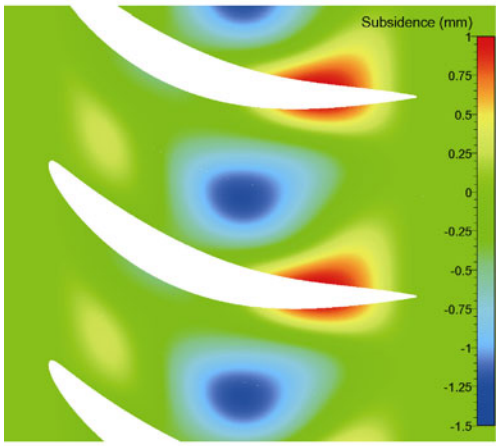

(b) End-Wall Profile Height Contours

Fig.3 Non-Axisymmetric Hub End-Wall Configuration (blue refers to concave curvature, red refers to convex curvature)

Results and Discussion

In order to verify the optimal compressor hub end-wall configuration (after 25 optimization cycles) and to provide insight into how non-axisymmetric hub end-wall increases the compressor performance, a coupled flow calculation through the subsonic compressor and non-axisymmetric hub end-wall were carried out using a state-of-the-art multi-block flow solver. Fig. 4 shows the overall impact of non-axisymmetric hub end-wall on the compressor total pressure ratio and isentropic efficiency map at 71 percent design speed. To show the validity of the numerical tool used in this paper, the measured performance characteristic of the compressor with the axisymmetric hub end-wall is also shown in Fig.4. It can be seen in Fig. 4 that the calculated compressor characteristic (with the axisymmetric hub end-wall) is in excellent agreement with the experimental data. Fig.4 also shows an impact of the non-axisymmetric hub end-wall configuration on the compressor total pressure ratio and isentropic efficiency. It can be observed from Fig.4 that the inclusion of non-axisymmetric hub end-wall gave increased pressure ratio and isentropic efficiency throughout the mass flow range compared to the baseline stage with the axisymmetric hub end-wall. The maximum efficiency increased by 2.04 points. In addition, the optimal compressor hub end-wall configuration has no detrimental effect on the compressor's stall margin.

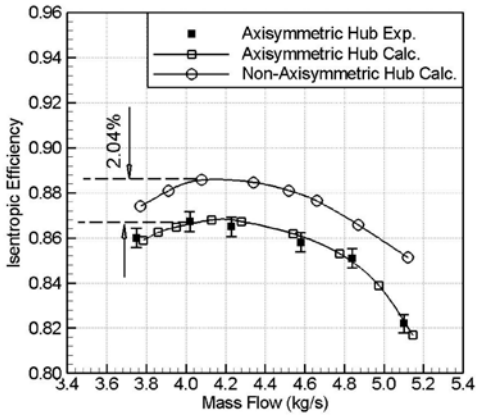

Fig.4 Comparison of the Compressor Performance Maps for the Baseline and Optimal Hub End-Wall Configurations

A comparison of the calculated span-wise distributions of the stage total pressure ratio, isentropic efficiency and absolute flow angle at peak efficiency condition are shown in Fig.5 for both the baseline and optimal compressor hub end-wall configurations. One can find from Fig.5 that the application of the non-axisymmetric hub contour causes a significant increase of the total pressure ratio and isentropic efficiency between 0% and 30% span, so the overall total pressure ratio and isentropic efficiency are increased as compared to the case with the axisymmetric hub end-wall. In addition, a reduction of absolute flow angle variations at the exit was also observed in Fig.5 (c) and the non-axisymmetric hub end-wall can result in about 5 degree decrease of flow angle near the hub end-wall at 10% span.

That is to say, the application of the non-axisymmetric hub contour has considerably reduced the under-turning of the flow which had been caused by the blockage of the hub-corner stall and the radial distributions of the stator exit flow parameter become uniform (increase uniformity in exit-flow angle), this resulted in a higher overall turning in the hub boundary layer.

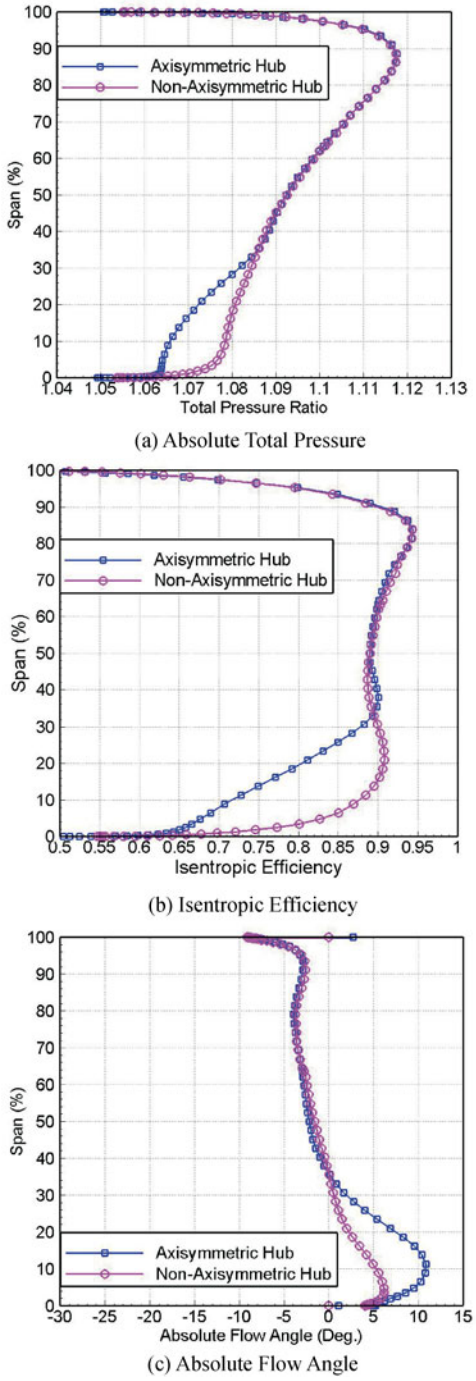

Fig.5 Comparison of the Radial Distribution of Circumferentially Averaged Outlet Flow Parameters at Stator Exit for the Baseline and Optimal Hub End-Wall Configurations

The static pressure coefficient, which was normalized by inlet total pressure, is shown along 5% span and 50% span for the baseline and optimal compressor hub end-wall configurations in Fig.6. As seen in Fig.6, the non-axisymmetric hub end-wall only affects the blade loading close to hub end-wall, which is consistent with the radial distributions of the stator exit flow parameters shown in Fig.5. Also, one can notice on the blade wall pressure distributions presented in Fig.6 that the non-axisymmetric contouring can redistribute vane load locally and delay the suction side boundary layer separation, which occurs further downstream in the optimized non-axisymmetric hub end-wall. It also reduces the detrimental negative incidence effects.

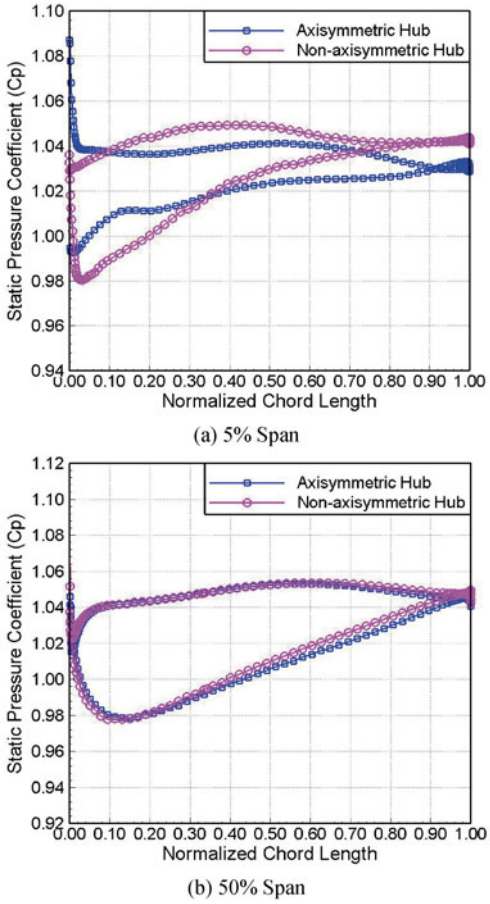

Fig.6 Comparison of Predicted Blade Loading at 5% Span and 50% Span for the Baseline and Optimal Hub End-Wall Configurations

The secondary flow vector plot and total pressure loss (CP*1) at several selected planes (50%, 75% and 100% axial chord) nearly normal to the vane root chord direction at peak efficiency operating condition, both with axisymmetric and non-axisymmetric hub end-wall, are compared in Fig.7. The focus lies on the very blade root in order to follow the development of the passage vortex. A secondary flow vector is defined in this paper as the difference vector between the local flow vector and an averaged flow vector. The total pressure loss was normalized by inlet total pressure, and the high loss region corresponds to the passage vortex core. Fig. 7 shows that the passage vortex has been fully developed at the 50%

axial chord which is originated from the pressure surface leg of the horseshoe vortex for the case with asymmetric hub end-wall, as the passage developing toward the trailing edge of the blade, the core of the passage vortex moves against the blade suction surface and hub end-wall, during this process the passage vortex strength and size increasing. However, one can find from Fig.7 that the non-axisymmetric hub end-wall have significant influences on the secondary flow structure near hub end-wall region, compared to the axisymmetric hub end-wall configuration, the formation and development of in-passage secondary flow has been delayed and consequently the passage vortex reduced in size and strength. From the total pressure loss distribution one can conclude that the contoured end-wall results in a significant total pressure loss reduction across the passage compared to the axisymmetric hub end-wall.

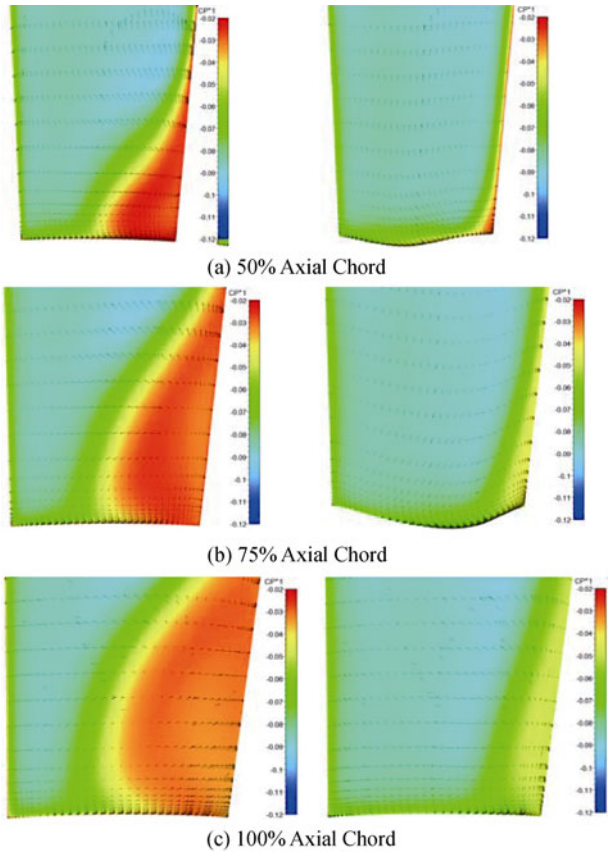

Fig.7 Comparison of Secondary Flow Vectors and Total Pressure Loss Coefficient Contours for the Baseline (left) and Optimal (right) Hub End-Wall Configurations

The distribution of blade suction surface limiting streamline patterns for the baseline and optimal compressor hub end-wall configurations are compared in Fig.8. For the case with the axisymmetric hub end-wall, one can notice from Fig.8 (a) that the suction surface separation line originates at about 10% chord from the leading edge at the suction surface/end-wall corner and terminates at the trailing edge at a distance also equivalent to about 90% of chord length from the end-wall. The separation and hub-corner stall could be significantly mitigated as shown in Fig.8 (b), by using the optimal non-axisymmetric hub end-wall configuration. Compared to the axisymmetric hub end-wall, the separation was delayed and the separation zone was greatly reduced, the prevention of this loss source explains the significant improvement in performance over a wide operating range.

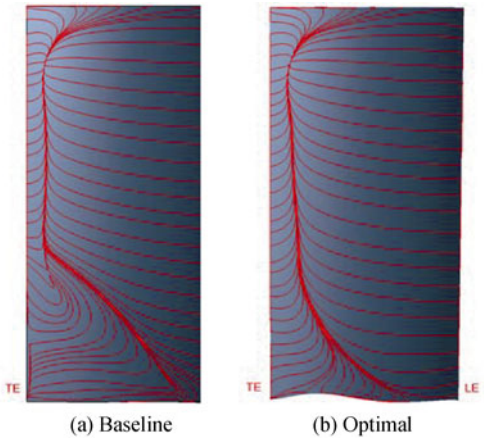

Fig.8 Comparison of Blade Suction Surface Limiting Streamline Patterns for the Baseline and Optimal Hub End-Wall Configurations

Evidence of supporting the predicted compressor performance improvements is further provided in Fig.9, which shows the contours of relative Mach number at 5% blade span for both the baseline and optimal compressor hub end-wall configurations at peak efficiency operation condition. Compared to the axisymmetric hub end-wall, the separation zone near the blade suction surface was significantly reduced and the flow characteristics of blade suction surface were greatly improved, as shown in Fig.9 (b), with the inclusion of optimal non-axisymmetric hub end-wall configuration.

Conclusions

In order to explore strategies for reducing secondary flows in blade passages through the use of end-wall contouring and to provide additional degrees of freedom for compressor geometric set-ups, a RANS flow solver has been used in conjunction with an automated multi-objective optimizer to minimize the secondary losses of a high subsonic axial-flow compressor stator. The effect of non-axisymmetric hub contouring on the compressor performance was quantified and the resulting flow phenomena and physics due to the modified end-wall surface

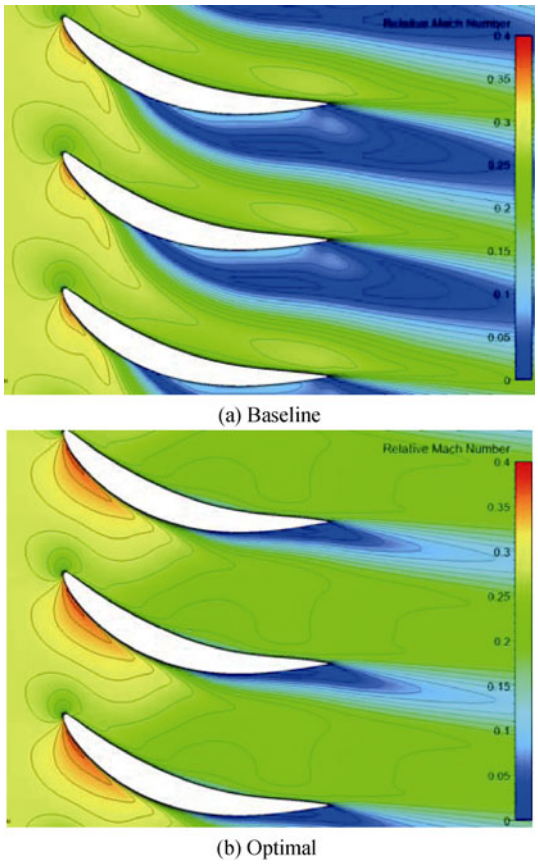

Fig.9 Comparison of Absolute Mach Number at 5% Blade Span for the Baseline and Optimal Hub End-Wall Configurations

were analyzed in details. The following conclusions can be drawn from this investigation.

(1) The results in this paper convincingly demonstrate significant reductions in aerodynamic loss with non-axisymmetric hub end-wall contouring and the non-axisymmetric contoured end-wall has shown its potential for compressor performance improvements. Based on CFD simulations, the optimal compressor hub end-wall configuration is expected to increase the peak efficiency by approximately 2.04 points and a slight increase of the total pressure ratio.

(2) The primary performance enhancement afforded by the non-axisymmetric hub end-wall is a result of the end-wall flow structure modification. Compared to the axisymmetric hub end-wall case, the non-axisymmetric hub end-wall configuration can reduce the size and strength of the passage secondary flows and delay the formation and development of in-passage secondary vortex by load redistribution, thereby results in a significant loss reduction.

Acknowledgments

Financial support for the work presented is provided by National Natural Science Foundation of China (Project No: 51176187), this support is greatly appreciated. Special thanks are also given to Mr. Tsukasa Yoshinaka, former Chief of Compressor Aerodynamics Department, Pratt & Whitney Canada and Vice President of Concepts NREC Inc., for his valuable guidance, supplements and review of the paper.

References

[1] Müller, R., Sauer, H., Vogeler, K. and Hoeger, M.: Influencing the Secondary Losses in Compressor Cascades by a Leading Edge Bulb Modification at the Endwall, ASME Paper GT2002-30442, Amsterdam, The Netherlands, (2002).

[2] Bergner J and Schiffer H P.: Experimental investigation of the Flow in a Forward Swept Transonic Compressor Rotor at Stall Inception. ASME Paper, GT-2007-27638, Montreal, Canada, (2007).

[3] Denton, J D and Xu, L.: The Effects of Lean and Sweep on Transonic Fan Performance. ASME Paper, GT-2002-30327, Amsterdam, The Netherlands, (2002).

[4] Müller, R., Vogeler, K., Sauer, H. and Hoeger, M.: End-wall Boundary Layer Control in Compressor Cascades, ASME Paper GT2004-53433, Vienna, Austria, (2004).

[5] Simon J. Gallimore, John J. et al.: The Use of Sweep and Dihedral in Multistage Axial Flow Compressor Blading - Part I: University Research and Methods Development, ASME Journal of Turbomachinery, Vol.124, No.4, pp521–533, (2002).

[6] Hoeger, M., Cardamone P. and Fottner, L.: Influence of Endwall Contouring on the Transonic Flow in a Compressor Blade, ASME Paper GT2002-30440, Amsterdam, The Netherlands, (2002).

[7] Müller, R., Vogeler, K., Sauer, H. and Hoeger, M.: End-wall Boundary Layer Control in Compressor Cascades, ASME Paper GT2004-53433, Vienna, Austria, (2004).

[8] Müller M W, Schiffer, H-P, Hah, C.: Effect of Circumferential Groove on the Performance of an Axial Single-Stage Transonic Compressor. ASME Paper GT-2007-27365, Montreal, Canada, (2007).

[9] Wilke, I, Kau, H-P and Brignole, G.: Numerically Aided Design of a High-efficient Casing Treatment for a Transonic Compressor. ASME Paper, GT-2005-68993, Reno-Tahoe, Nevada, USA, (2005).

[10] Shabbir, A, Adamczyk, J J.: Flow Mechanism for Stall Margin Improvement due to Circumferential Casing Grooves on Axial Compressors. ASME Paper, GT-2004-53903, Vienna, Austria, (2004).

[11] Brennan, G., Harvey, N., W.,Rose, M., G., Fomison, N. and Taylor, M., D.: Improving the Efficiency of the

TRENT 500 HP Turbine using Non-axisymmetric Endwalls. Part 1: Turbine Design, ASME Paper 2001-GT-0444, New Orleans, Louisiana, USA, (2001).

[12] Ingram, G. and Gregory-Smith, D.: The Effect of Endwall Profiling on Secondary Flow and Loss Development in a Turbine Cascade, ASME Paper GT-2002-30339, Amsterdam, The Netherlands, (2002).

[13] Harvey, N., W., Brennan, G., Newman D., A. and Rose, M., G.: Improving Turbine Efficiency using Non-axisymmetric Endwalls: Validation in the Multi-row Environment and with Low Aspect Ratio Blading, ASME Paper GT-2002-30337, Amsterdam, The Netherlands, (2002).

[14] Dorfner, C., Eberhard, N. and Voss, C.: Axis-asymmetric Profiled Endwall Design using Multi-objective Optimization Linked with 3D RANS-flow-simulations, ASME Paper GT2007-27268, Montreal, Canada, (2007).

[15] Harvey, N., W.: Some Effects of Non-axisymmetric End Wall Profiling on Axial Flow Compressor Aerodynamics. Part I: Linear Cascade Investigation, ASME Paper GT2008-50990, Berlin, Germany, (2008).

[16] Harvey, N., W. and Offord, T., P.: Some Effects of Non-axisymmetric End Wall Profiling on Axial Flow Compressor Aerodynamics. Part II: Multi-stage HPC CFD Study, ASME Paper GT2008-50991, Berlin, Germany, (2008).

[17] Xingen Lu, Junqiang Zhu, Wuli Chu: Numerical and Experimental Investigation of Stepped Tip Gap Effects on a Subsonic Axial-flow Compressor Rotor. Proceedings of the Institution of Mechanical Engineers Part A: Journal of Power and Energy. Vol.219, No.A8, pp605-615, (2005).

[18] X. Lu, W. Chu, J. Zhu, and Z. Tong: Numerical and Experimental Investigations of Steady Micro-Tip Injection on a Subsonic Axial-Flow Compressor Rotor, International Journal of Rotating Machinery, Article ID 71034, 11 pages, doi:10.1155/IJRM/ 2006/71034, (2006).

[19] Xingen Lu, Wuli Chu, Junqiang Zhu: Numerical Investigations of the Coupled Flow through a Subsonic Compressor Rotor and Axial Skewed Slot, ASME Journal of Turbomachinery, Vol.131, No.1, pp1−8, (2009).

[20] NUMECA's Flow Integrated Environment for Turbomachinery and Internal Flows, User Manual, Version 6.1−1, (2003).